Fabrication and Characterization of 60 Channel Microelectrode Arrays for Recording and Stimulation from Cardiac Cells in Culture

Vanessa Pereira Gomes[1,2], Angelica Denardi de Barros[2], João-Batista Destro-Filho[3], Sergio Martinoia[4], Alberto Pasquarelli[5], and Jacobus Willibrordus Swart[1,2]

[1]School of Electr. & Comput. Eng., State University of Campinas, Campinas, Brazil
[2]Center of Semiconductor Components and Nanotechnologies, State University of Campinas, Campinas, Brazil
[3]School of Electr. Eng., Federal University of Uberlândia, Uberlândia, Brazil
[4]Department of Inform.,Bioeng., Robotics and Systems Eng., University of Genoa, Genoa, Italy
[5]Institute of Electron Devices and Circuits, Ulm University, Ulm, Germany
e-mail: pgomes.vanessa@gmail.com

ABSTRACT

Stimulation and recording of nerve cells is a procedure used for several applications, such as clinical therapies, study of basic neuroscience, and neural prostheses. Microtechnology and advances in material science have allowed to produce more sophisticated devices and with more functions. This paper focuses on the fabrication of planar 60 – channel Microelectrode Arrays (MEAs). The electrical characterization of the noise level from the TiN electrodes showed good sensitivity to noise, compatible with commercial systems. These electrodes received an artificial electrocardiogram signal (ECG) from a function generator and registered the same input signal but with lower amplitude. Finally, both cyclic voltammetry curves of the produced MEA and the commercial MEA exhibited similar shape, but the current density of the first one was significantly higher than in MCS – MEA, with an order difference of magnitude.

Index Terms: Microelectrodes; Microfabrication; Cell; Recording; Stimulation.

I. INTRODUCTION

Microelectrode Array (MEA), a tool available for both pharmacological applications [1] and electrophysiological measurements [2], was initially a two – dimensional arrangement designed only to extracellular stimulation and monitoring of the electrical activity of electrogenic cells (as neurons of the central nervous system, peripheral muscle cells, and cardiac tissues of humans and animals), tissue slices, and cultures [3]. However, it has been widely used in neuroscience to record spikes from brain slices [4], dissociated neuronal [5], retinas [6], and cardiomyocytes cultures [7].

MEA has several advantages, such as non – invasively, multisite recording of cell potentials (up to tens of channels), allowing long – term recordings under properly maintenance conditions (from several hours up to months or even a year), and it is also capable to stimulate by applying potential on the electrodes [8, 9].

As the use of MEAs requires being in contact with a quite corrosive medium (human body), the choice of materials is an important step. In general, MEAs must exhibit [10]: biocompatibility (i. e., they must not show any toxic effect or cause immune res-ponse in vivo on cells or tissue culture since they are in direct contact in order to provide good adhesion, with small low power consumption to avoid the production of damage to biological tissue), good electrical characteristics (because electrodes and contact pads properties influence the ability of measuring small signal amplitudes with good signal to noise ratio), electrodes with safe charge injection capacity, and low cost (as standard MEA size is about 5 cm X 5 cm).

The present paper reports the fabrication of planar sixty channel MEAs (steps, materials e procedures) and their characterization. We have successfully developed all steps in order to fabricate the whole MEA in Brazil, so that it was done with 100% national technology. Testing results point out that the device yields very good performance, close to standard commercial MEAs.

II. METHODOLOGY

Microelectrode arrays were manufactured using standard microfabrication technology. The array consists of 60 round, flat electrodes, connected to contact

pads (4.84 mm², and separated by 0.2 mm) by the tracks (with a width of 40μm at the electrodes) as shown in Fig. 1.

MEAs' structure can be subdivided into 5 basic parts: substrate, interlayer, electrodes/ tracks/ contact pads, insulation and ring and it was achieved through conventional silicon microfabrication processing using glass as substrate. As shown in Fig. 1, the microfabrication process was divided into 5 steps, after the cleaning of the substrates. The first step (step I) consists in the deposition of an insulator interlayer between glass and metal (which will form the electrodes, tracks and contact pads through lift – off technique) (step II). Next there is the deposition of the first (stage III) and second (step IV) passivation layer. To complete the device, final components are placed, such as ring and contact pins (step V).

Next each step is discussed in greater details.

(a)

(b)

Figure 1. (a) Manufactured MEA; (b) MEA fabrication process at Center of Semiconductor Components and Nanotechnologies (UNICAMP). The fabrication process is subdivided into 5 steps: (I) deposition of an insulator interlayer between glass and conductor, (II) implementation of the electrodes, tracks and contact pads, (III) first insulation layer manufacturing, (IV) second insulation layer deposition, and (V) final components placement, such as ring and contact pins.

A. Step I

Various materials can be employed as substrate. Among the most commonly used in MEAs include silicon (Si), glass, quartz, and sapphire [10 – 13]. For rigid electrodes facing neural applications, silicon and glass are the most common materials. However, due to some characteristics unsuitable for this application, such as optical transparency, chemical inertness, and electrical properties, silicon has been gradually replaced by quartz and glass [14, 15].

Among the physical characteristics that define the best choice for the substrate, there may be mentioned rates of expansion and thermal conductivity, melting point, density and hardness. Because of the need to work with a transparent substrate and suitable melting point, quartz and glass are shown as the best options. Therefore, this work uses glass as substrate, which is one of the most popular materials for MEAs due to their qualities, such as chemical resistance, thermal stability, optical transparency, electrical insulation (minimizing some parasitic elements, such as interconnect – electrolyte and interconnect – substrate capacitances, typically found on silicon substrates) and biocompatibility [16, 17].

First step starts with the cleaning of the substrate material to avoid the accumulation of impurities at the interface with the interlayer. Cleaning was performed by dipping the substrate in detergent solution (EXTRAN MA02 3% v/v from Merk), and next in water, hydrogen peroxide (30% from UltraPure Solutions, Inc.) and ammonium hydroxide (29% from JT Baker) solution with a ratio of 5: 1: 1 for 15 minutes.

Although it is not a compulsory practice, and many studies do not consider it, we consider interesting to create an interlayer between substrate and conductor. This additional step is important to minimize the action of possible contaminants arising from the substrate, that could damage the device, and to prepare it for the coming processes, improving adhesion between substrate and metal layer.

Therefore, next step consists in depositing the interlayer material. Most common materials for insulation are silicon dioxide (SiO_2), silicon nitride (Si_3N_4), and amorphous silicon (α – Si) [10, 14, 17] (see Table 1). In general, these materials are deposited with thickness up to 100 nm, attempting to preserve the transparency of the substrate [17 – 19]. In this work, silicon dioxide was chosen as interlayer material due to its transparency on glass substrate. Deposition of 50 nm interlayer was carry out by Sputtering (from ULVAC MCH9000).
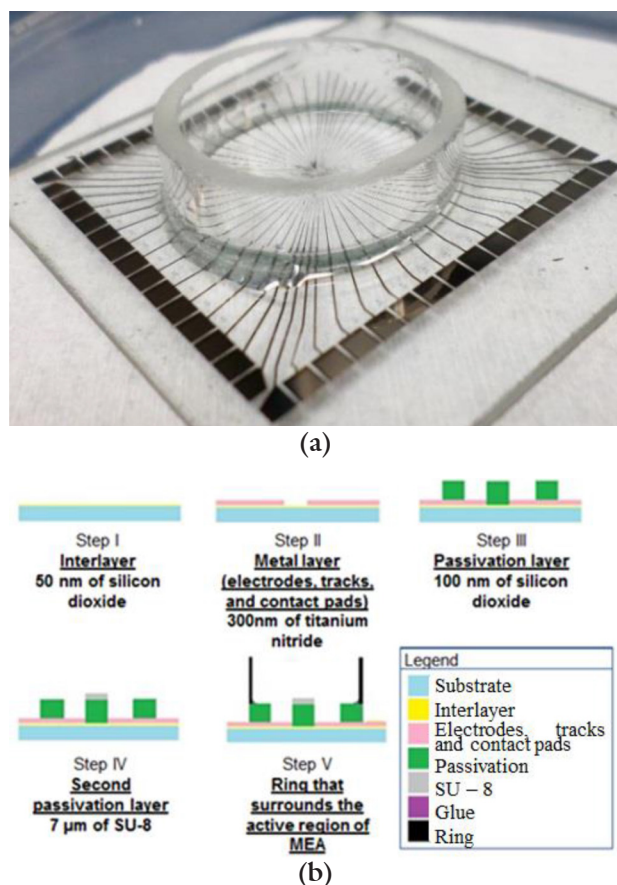
Table I. Material properties

	SiO$_2$	Si$_3$N$_4$	Si	References
Thermal expansion (x 10^{-6}/ºC)	0.55	0.8	2.33	[22]
Resistivity in 25ºC (Ωcm)	10^{14} - 10^{16}	~10^{14}	2.3 x 10^5	[23, 24]
Dielectric constant	3.9	7	11.9	[25, 26]
Thermal conductivity (WºC/ cm)	0.014	0.19	1.57	[22]
Penetration resistance (Kg/ mm²)	820	3486	850	[22]
Rigidity (10^{12}dinas/ cm²)	0.73	3.85	1.9	[22]
Refractive index	1.47	2.3	3.95 ± 0.05 (α – Si)	[27, 28]
Density (g/ cm³ or ton/m³)	2.5	3.1	2.3	[22]

B. Step II

After cleaning and formation of the interlayer, next phase is electrode, track and contact pad production, by depositing a conductive material.

This step includes the lithography process in order to define electrodes, tracks, and contact pads, after sputtering deposition of the conductive material.

A wide variety of materials, such as nanocrystalline diamond, gold, platinum (Pt), platinum – iridium alloy, tantalum, activated iridium oxide films (IrOx), electrically conducting polymer, poly(ethylenedioxythiophene), graphene and titanium nitride (TiN) [17 – 19] can be applied in this step. Among these materials, titanium nitride shows low impedance, good biocompatibility, excellent stability and a large charge injection capacity (approximately 1 mCcm^{-2}) which makes it a good option for devices that monitor and stimulate long – term biological activity with low noise [19, 20]. Thus, this material was chosen to compose the conductive parts of the MEA chip.

Electrodes are round and their diameters depend on the application and can vary widely, ranging from 10 μm to 160 micrometers [17]. However, since cell diameters for which this MEA is designed can reach 30 – 40 μm (neurons from dorsal root ganglion (DRG) from male Wistar rats) [21], the diameter of the electrodes of this work is 30 μm.

In addition to neurons in brain slices, in general, signal sources are within a radius of 30 μm around the electrode center and can be registered up to 100 micrometers [18], which is within range of a MEA electrode produced here, since the spacing is 200 μm. This distance is also sufficient to obtain a good resolution and sensitivity over the short period in which a release of adrenalin by chromaffin cells, neuroendocrine cells found in the medulla of the adrenal gland [18].

Lift – off was adopted to define the conductive region and 300 nm TiN layer with resistivity of 150 $\mu\Omega$.cm was deposited by Sputtering.

C. Step III

In order to perform electrical measurements in liquid media, a passivation layer is required above conductive electrodes. This is a critical step during MEA development and usually employs silicon nitride, silicon dioxide and silicon dioxide – silicon nitride – silicon dioxide composite [10, 20, 17].

Capacitance (Cp) can be obtained through an expression that correlates the main parameters that influence the amplitude of this variable, which is known as Sakurai – Tamary equation (Eq. 1) [17]:

$$C_p = \frac{1.15\varepsilon_0\varepsilon_r LW}{d} + 2.80\varepsilon_0\varepsilon_r L(\frac{t}{d})^{0.222} \qquad (1)$$

Where ε_0 is space permissivity, ε_r is insulating material permissivity, d is the thickness of the insulation layer, and L, W and t, are the length, width and thickness of the track, respectively.

Consequently, capacitance is determined by the material used in the insulation layer, its thickness, and geometric area of the track.

This process aims to prevent that the electrolytes present in solution may infiltrate in this passivation layer, generating pin holes, and finally reaching the electrodes layer, effect that is not desired [17].

The definition of the insulating layer was made by lift – off process, with Sputtering deposition of 100 nm of silicon dioxide.

D. Step IV

Often, this single insulating silicon dioxide layer is not enough to block pin holes creation at the non – sensitive region of MEA, which could affect signal capture by electrodes. In order to avoid it, so the electrolyte can reach conductive surface from any direction except openings (electrodes), it is appropriate to

add another passivating layer that does not hinder the transparency of the device.

Therefore, the material chosen in this work was SU – 8 10 from MicroChem, a biocompatible and transparent material, with *7 μ*m thick.

E. Step V

Final step of MEA manufacturing requires the definition of a ring that surrounds the active region of MEA (i. e., electrodes zone), allowing to perform electrochemical measurements and to ensure that culture medium doesn't evaporate too fast during cell experiments, keeping a sufficient volume of biological material [17]. For this purpose, a ring, which can hold up to about 800 *μ*L solution [18], was made with glass. Rings had inner and outer diameters of 2.2cm and 2.6 cm, respectively, and they were fixed on the MEA surface with biocompatible glue.

III. RESULTS AND DISCUSSION

Electrical characterization was carry out at Center of Semiconductor Components and Nanotechnologies at State

University of Campinas, University of Genoa and Universi-ty of Ulm. Tests were classified in: (A) analysis of the noise level (amplitude of the potential recorded with adding standard saline solution), (B) electrical stimulation, and (C) electrode test (cyclic voltammetry and impedance spectroscopy). These techniques are briefly described below, as well as the results obtained.

A. Noise Level

Neurons activity is captured as an extracellular potential, or action potentials, when electrodes, which are close to the target neuron, detect the firing of an action potential of a single neuron. Therefore, a good quality recording of a single neural unit is obtained with a signal – to – noise ratio of approximately 5: 1 or even higher. However, although usually much of this noise come from the neural noise, i. e. a multitude of workstations that cannot be observed individually, it is also influenced by the electrode impedance. Furthermore, the combination of a high electrode impedance (producing a lower signal – to – noise ratio) with the capacitance between electrode and amplifier minimizes the response of the electrode in high frequency [19].

Based on this, noise level experiment was performed. This test consists in recording electrical potential in the MEA, and permits to identify which electrodes work properly. To make this classification,

obtained results for the manufactured MEA were compared with those presented by the standard MEA from *MultiChannel Systems* (MCS).

Initially, the reservoir surrounded by the ring (active area) was filled with a medium composed of two culture media (NeuroBasal and B27), totaling 1 mL of solution.

Once placed the culture medium in the reservoir, MEA is coupled to the MultiChannel Systems standard socket [18]. Then it is connected to the amplifier, with the reference electrode connected to the ground channel of the amplifier. Sampling frequency of the measurement was 10 kHz, and total gain of 1000 (between the sign at the entrance of the microelectrodes and the final output after all amplifications), without any digital filtering and inside a Faraday cage.

This experiment records just the thermal noise of the amplifiers, once there was no connected biological culture in the reservoir. Same procedure was performed for a new standard MultiChannel device.

Best results showed low amplitude noise, with a peak – to – peak potential (V_{p-p}) equal to $10\,\mu V$ when tested with a random waveform. This result is compatible with commercial MEA [18]. In this context, most of the working TiN electrodes have showed very good sensitivity to noise, similar to the standard MCS, with amplitudes ranging from -8 to 10 μV, i. e., 20 μV_{p-p} (see Fig. 2).

There are several reasons to explain the occurrence of high levels of noise in unit electrodes. It may occur due to problems in the external measuring system or MEA. Among the most common problems are: (a) damage to the amplifier contact pin; (b) lack of reference electrode and shielding during recording (that can generate extremely high amplitudes signal, saturating the amplifier); (c) signal lack or strange behavior,
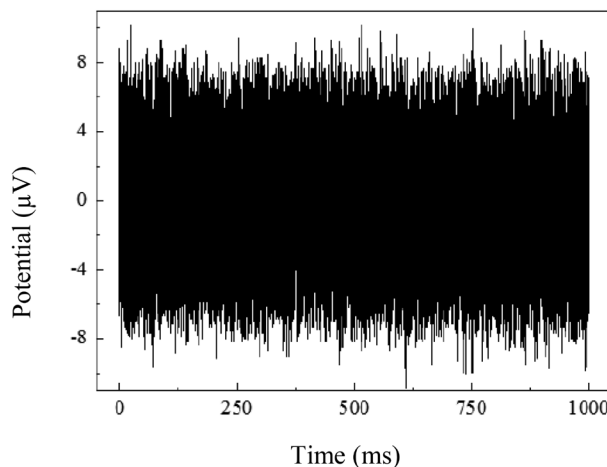

Figure 2. Recorded signal (μV) in one electrode in our MEA as a function of time. As it can be seen, the electrode showed very good sensitivity to noise, with amplitude ranging from -8 to 10 μV.

which may occur by MEA use; (d) contact pads contamination (and this is a solvable problem because only a cleaning with pure alcohol is enough); and, finally, (e) irreversible damage to the electrode or contact pad. The latter can be observed from the coloring modification of the sensor [18].

Noise level comes both from amplification system and from MEA device. Regarding the device, signal amplitude depends on two factors. It is influenced by size and material that makes up the electrodes. The smaller the diameter of the electrode, the greater the noise.

For titanium nitride electrodes, which have a rough surface, impedance and noise are lower than those found in electrodes with same diameter made of other materials such as platinum. Initial noise can be higher of MEA is composed of hydrophobic materials and one way to solve this problem is to create a hydrophilic surface, which is possible with the adoption of appropriate materials, such as titanium nitride [18].

To estimate the noise level contained in the recorded signal was obtained the RMS value for a non – defective microelectrode of our MEA. For the raw signal (unfiltered), the value found was 2.6 microvolts for the manufactured MEA. This result is satisfactory, since, to consider the microelectrode as functional, this parameter must be within the range of 2.5 to 8 microvolts [18].

B. Electrical Stimulation Test

Electrical stimulation test evaluates the recording ability of the electrodes and observes whether the output signal is similar to the input signal utilized to test.

Tested electrodes were the same which exhibited good results in noise test. Other electrodes were disconnected.

Experimental setup in this experiment was similar to the setup described in section III – A, but in addition a cardiac signal was introduced in the culture medium. The signal tested in this case was an artificial electrocardiogram signal (ECG), which simulates real cardiac potential generated by cardiac cells. Therefore, it was injected an artificial ECG signal that consists of a peak – to – peak amplitude of 0.5mV with a cardiac cycle repetition frequency ranging from 3 to 23 Hz in the culture medium described in section III – A.

Fig. 3 shows the amplification of a part of the electrical potential recorded as function of time for the microfabricated MEA for one tested electrode. It was possible registering a quite close signal to the injected ECG signal in the culture medium.

Based on the results of Fig. 3, it is clear that it was possible to register a very close ECG signal injected by the function generator in the culture medium.
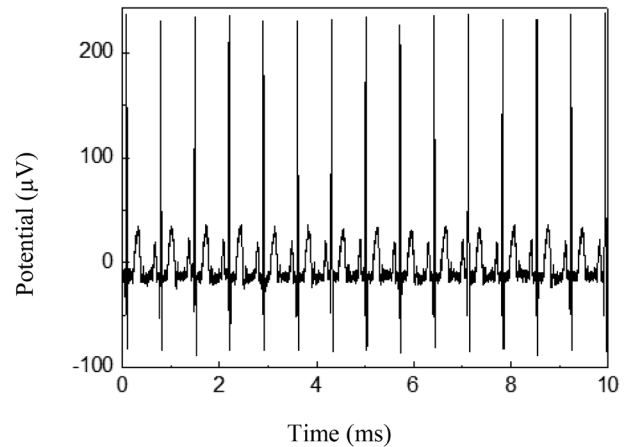

Figure 3. Stimulation results. The signal represents the electrical activity in an electrode, recorded during stimulation by means of an artificial electrocardiogram signal generator. This signal is about 0,33 mVp-p, as expected, as there are losses in the cables and coupling between the culture medium and electrodes. These levels are still reasonable for biological experiments.

The record showed a lower range (range of approximately 0.33 mV_{p-p}), as expected, due to losses in the cables and the coupling between the culture medium and the electrodes. Even though, registered levels are still reasonable for biological experiments. In general, electrical stimulation wear all electrodes, especially if applied over a long – term. The impact on their performance depends on the electrode employed and the stimulus applied. During a pulse, electrodes behave like a capacitor, because the charge that is transmitted by the voltage generator cannot go to the inverse way, i. e., from electrodes to the generator. This is due to elevated output impedance and hence all charge is maintained on the electrode. To discharge it is necessary a long time after stimulation. Thus, stimulation artefacts interfere in signal capture and electrodes progressively deteriorate due to electrolysis. To avoid this situation, an appropriate protocol to the MEA should be used such that electrodes are able to discharge after stimulation [18].

Unlike platinum, titanium nitride cannot be positively charged, because this action will lead to electrolysis. Consequently, the stimulation is performed introducing negative voltages, since positive voltages will briefly positively charge even if it is discharged at the end of the pulse. Therefore, the recommendation is to apply negative monophasic voltage stimuli, which ensures that the amplitude of the stimulating electrode voltage is zero and this allows that the electrode is discharged at the end of the pulse. However, when stimulation is performed by current, best way is biphasic, with the first phase negative to prevent positive net charge on the electrode [18].

For neural applications, stimulation pulse by voltage must be less than 1 V, usually from -100 mV to

-900 mV, with pulse duration of 100 μs to 500 μs. In this range, dam-age to electrodes and cells are avoided [29]. Cardiomyocytes, however, require greater excitement and for a longer period of time. It is suggested apply -2 V for 2 ms. The problem is that standard electrodes (made of TiN with 30μm in diameter) do not support pulse of this magnitude. Therefore, it becomes necessary to use MEAs with larger diameter electrodes [30].

Based on this and considering the signal injected into the culture medium during stimulation test, it would be interesting to apply only negative potentials, because otherwise MEA will have a very small lifetime. Furthermore, improvements may be employed to obtain signals which can be registered closer to the injected signal.

As previously mentioned, a factor that exerts a significant contribution are the cables that connect the socket of the MEA to the external measurement system. One way to solve this problem is to use shielded cables, which thereby minimize noise and make the results recorded more similar to the introduced [18].

C. Cyclic Voltammetry

Cyclic voltammetry is an electrochemical method in which the information about an analyte is obtained by measuring the current – i – that flows between counter and work electrodes as a function of applied voltage using triangular waveform for excitation in the test electrode, related to the reference electrode. As the reference electrode potential is stable, the measured voltage only reflects the change of the test electrode potential. Therefore, this measurement provides the driving force of the reactions that take place in the test electrode while current is proportional to the rate of these reactions [30, 31].

Thus, in this work, this technique was applied with the primary purpose of detecting whether electrodes are working properly or they are defective and hence cannot register and/ or stimulate.

Initially, it injects a potential value that causes no reduction in the solution. Then, this signal varies until it reaches negative potentials (cathodic). At this point, the current decreases and this is equivalent to the level of reduction processes in the solution. When it reaches a moment at which no further reduction occur, the potential varies in the opposite direction until returns to the initial value. If this reaction is reversible, products generated in the first potential variation and that are close to the surface of the electrode will oxide, which causes a new peak (symmetrical to the first peak) [31, 32].

Fig. 4 shows cyclic voltammetry curves obtained for the fabricated MEA (Fig. 4(a)) and MCS – MEA (Fig. 4(b)), respectively.
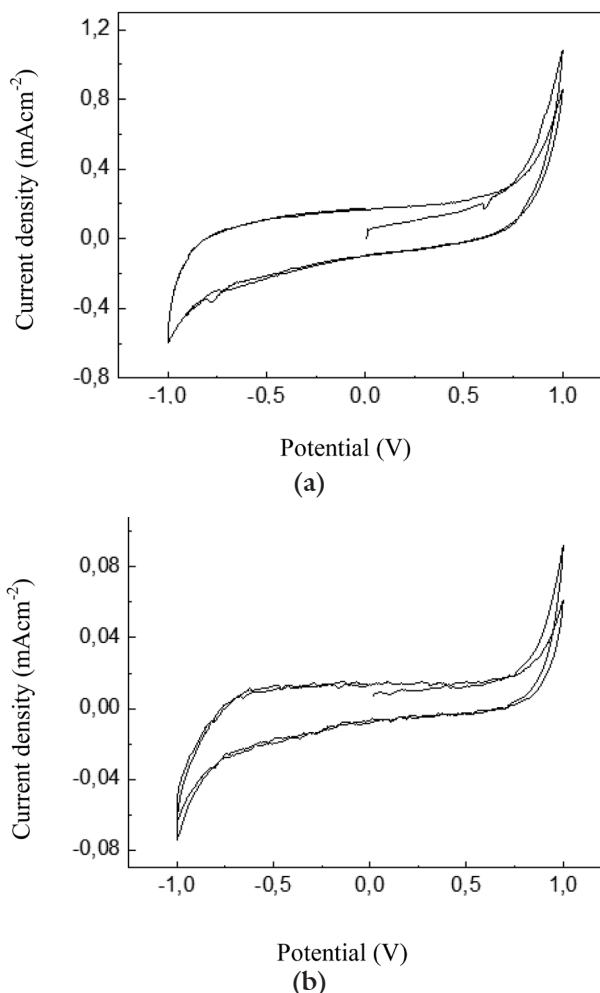

Figure 4. Cyclic voltammetry. (a) Manufactured MEA, and (b) MCS – MEA. Both CV curves are similar with regard to its shape, but the current density in our MEA was significantly higher than that of standard commercial MEA, so that the difference was about one order of magnitude.

Despite the similarities in the format of the curves, the current density in the produced MEA was significantly higher than that of commercial MEA (with an order difference of magnitude).

Another important data that cyclic voltammetry test provides is Cathodic Charge Storage Capacity (CSCc) of the stimulation electrodes, which basically measures the total amount of charge available during a stimulation pulse [19]. CSCc is calculated as the integral of the cathodic current (negative current) with respect to time in a cyclic voltammogram with low scan rate over a range that is within the electrolysis window of water [33].

The difference in the curve formats shown in Fig. 4 was confirmed by CSCc. This data was obtained for our MEA and MEA from MultiChannel Systems. Found values were 0.63 mC.cm^{-2} and 0.05 mC.cm^{-2}, respectively, for a potential window of -1 V to +1 V.

The difference in the results may be attributed mainly to the different thickness of the conductive layer, since both our MEA and MEA from MultiChannel Systems present electrodes with 30 μm in diameter made of titanium nitride, and with interelectrode distance of 200 μm.

Microelectrodes (with area smaller than 10,000 μm^2) generally can show a charge density in a wide range varying from 0.2 to 3.5 mC.cm^{-2} [19]. Within the group of materials which operate via faradaic mechanism, platinum/ platinum alloys, activated iridium oxide and thermal iridium oxide exhibit charge injection limit ranging from 0.05 – 0.15 mC.cm^{-2}, 1 – 5 mC.cm^{-2}, and ~1 mC.cm^{-2}, respectively, while in capacitive materials, such as tantalum/ tantalum oxide and titanium nitride, these values were ~0.5 mC.cm^{-2}, and ~1 mC.cm^{-2}, respectively, with safe potential window of -0.9 V to +0.9 V [19]. However, charge injection limit was much higher. Values varied from 2.2 – 3.5mC. cm^{-2}, at a potential window of -1 V to +1.2 V [34].

Although obtained charge injection threshold for TiN electrode by Cogan (2008) [19] is 1 mC.cm^{-2}, CSC was 0.25 mC.cm^{-2}. Calculated CSCc values by Weiland et al. (2002) [35] and Aryan et al. (2011) [36] were 0.55mC.cm^{-2}, with potential window of -0.6 V to +0.8 V and 0.2mC.cm^{-2}, with potential window of -1 V to +1 V, respectively.

Consequently, the values obtained for produced MEA in this work are within the expected range and are higher than those found in the studies cited. Furthermore, there is a plateau region in all TiN electrodes measured in the cathodic scanning phase (ranging from approximately -0.65 V to +0.65 V for our MEA and -0.61 V to +0.69 V for MEA from MultiChannel Systems). This behavior is present due to hydrogen absorption that occurs before its release, which is similar to the cathodic reaction in platinum electrodes. After this interval there is an increase in the cathodic current and it represents therefore the evolution phase of gas hydrogen [34].

D. Impedance Spectroscopy

Another widely used technique for the electrical characterization of the MEA electrodes is Impedance Spectroscopy (IS), whose result allows setting whether an electrode is able to stimulate and record signals and, it is an interesting method for verifying in vivo. Moreover, it can also be used to study the tissues properties and electrical characteristics between electrode and solution interface [19, 36].

This technique works as follows: a unit frequency sinusoidal excitation is applied (which may be by voltage or current) to the electrode and the resulting current in this given frequency is measured, allowing to obtain both electrical impedance and phase angle (real and imaginary parts of impedance).

A wide range of frequencies can be employed, being typically between <1 Hz and 10^5 Hz, with a small excitation magnitude so that current response versus voltage is obtained at each frequency. Excitation values can vary between ~10 mV and 50 mV [19].

In general, impedance is obtained with injection of a small potential AC (alternating current) which can be, for example, a sinusoidal excitation in the electrochemical cell. Thus, the expression as a function of time is given by [37]:

$$E_t = E_0\sin(\omega t) \qquad (2)$$

Where E_t and E_0 are the potential at the time t and signal amplitude, with ω as radial frequency (radians/ second), which can be found as a function of frequency f (in Hertz) as in Eq. 3 [37]:

$$\omega = 2\pi f \qquad (3)$$

Thus, the resulting signal (I_t) to a linear system has an amplitude I_0 and is shifted in phase (Φ) as shown in Eq. 4 [37]:

$$I_t = I_0\sin(\omega t + \Phi) \qquad (4)$$

Therefore, impedance (Z) as a function of the magnitude (Z_0) and phase shift (Φ) can be found using a similar expression to the Ohm's law. Then, [37]:

$$Z = \frac{E_t}{I_t} = \frac{E_0\sin(\omega t)}{I_0\sin(\omega t + \Phi)} = Z_0\frac{\sin(\omega t)}{\sin(\omega t + \Phi)} \qquad (5)$$

Most used forms to exhibit this result have been Bode diagram of the absolute value of Z (or |Z|) as a function of the frequency, and Nyquist diagram (imaginary component or capacitive impedance (Z') as a function of the real component of the resistive impedance (Z)). It is interesting to note that in Nyquist diagram, each point means an impedance at a single frequency.

Related to an equivalent circuit modeling, although some electrochemical cells can present only one component, most cells employ elements that can be arranged in series and parallel.

Resulting equivalent circuit utilized in this work is illustrated in Fig. 5, whose components are Z_{CEP} (or Constant Element Phase, representing a non – faradaic impedance of the interface capacitance or polarization capacitance, and may appear due to some electrode surface roughness and describes satisfactorily the electrode – electrolyte interface studied in this work), R_{CT} (Charge Transfer Resistance, due to moving charge in the electrode – electrolyte interface), and R_S (Solution Resistance) [16, 37].
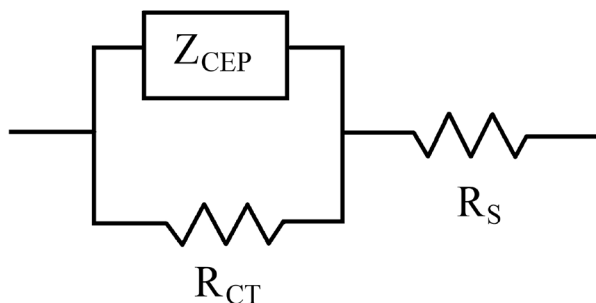
Figure 5. Equivalent model utilized in Impedance Spectroscopy test in MEAs, whose components are Z_{CEP} (Constant Element Phase, representing an impedance of the interface capacitance or polarization capacitance), R_{CT} (Charge Transfer Resistance) and R_S (Solution Resistance) [16].

Figure 6. Results from Impedance Spectroscopy measures referring to a microelectrode from our MEA. Real impedance (black symbol) and imaginary impedance (white symbol) curves are plotted as a function of frequency logarithm. Initially, at low frequencies, impedance is high and close to TiN, decreasing as the frequency is increased.

Impedance Z_{CEP}, which is the non – faradaic impedance resulting from the interface capacitance (polarization), is obtained using Eq. 6 [16]:

$$Z_{CEP}(\omega) = 1 / (j\omega Q)^n \qquad (6)$$

Where Q represents the magnitude of Z_{CEP}, n, the heterogeneities on the surface ($0 \leq n \leq 1$, where n equal to 1 indicates a purely capacitive surface), and with $\omega = 2\pi f$. The charge transfer solution resistances (resistance between working and reference electrodes) can be obtained by Eq. 7 and 8 [16]:

$$R_{CT} = R_T / (J_0 zF) \qquad (7)$$

$$R_S = \rho / 4r \qquad (8)$$

Where RT/ F = 26 mV at 298 K, J_0 is the current magnitude flowing through electrode – electrolyte interface in the equilibrium situation (reduction current with the same module and direction opposite to oxidation), z is the number of electrons involved in the reduction – oxidation reaction, ρ is the solution resistivity (72 Ωcm for physiological saline) and r is the electrode radius [16].

Since we adopt TiN electrodes of 30 μm in diameter in this work, then R_S and R_{CT} are equivalent to 3×10^5 Ω and 12×10^3 Ω, respectively, and, therefore, the curves of the impedance module and phase versus frequency expected for IS test in MEA are shown in Fig. 6 [16].

In order to obtain Fig. 6, MEA is coupled to the socket which contains connectors. Stimulation electrodes (counter electrodes), placed directly on the culture medium, received the signal through a wire (platinum), which, in turn, leads to stimulation produced by a very slow amplitude stimulation generator. Other wire (made of silver) corresponds to the reference electrode. Finally, a third wire, which registers the
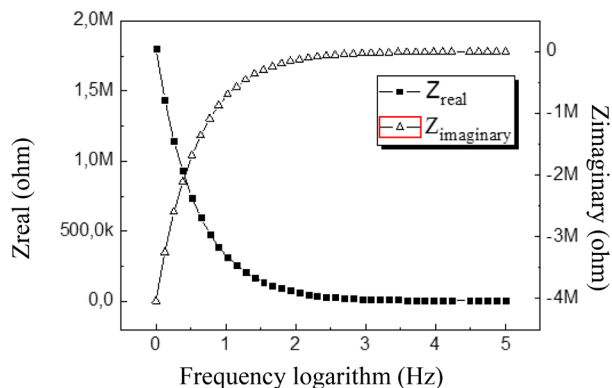
stimulation (connected to a potentiostat, device that actually performs the signal recording) is coupled to a single terminal (the latter associated to a microelectrode, called sensor electrode), whose signal is carried by the fourth ca –ble (connected to the working electrode) and the third wire to the computer, through an A/D interface.

Once placed the MEA in the socket and deposited the culture medium PBS (2,5 – 3 mL) in the region inside the ring, the electrode scheme is mounted. And thus this set is connected to the main apparatus, which is connected to other equipment. Usually, stimuli generator and a potentiostat require any initial calibration, in accordance with the operating rules specified in their technical documentation. Measurements are then performed with a Faraday cage, which is made of stainless steel, fully closed.

Initially, third wire is connected to one of MEA microelectrodes analyzed through tips connecting the socket terminals to fourth and third wires. Faraday cage is closed and, through the computer system, stimulus generator (PARSTAT 2273) is trigged. This device will induce microvoltage and/ or microcurrent of very low amplitude in the culture medium. Such stimuli are registered by the microelectrode under review, which induced signal is recorded in the computer system. From this point, it is analyzed microelectrode by microelectrode at MEA. The goal is to draw the Bode plot of each to different frequencies (1 Hz – 100kHz), generating the curves shown in Fig. 6. Procedure is repeated sixty times, until all microelectrodes are studied and their diagrams drawn.

Initially, at low frequencies, both impedance module and phase are high to TiN, decreasing as the frequency is increased. At low frequencies, phase tends to -80° for TiN.

From measured real and imaginary impedance values for the electrode, the module values of this impedance and phase angle as a function of applied frequency could be obtained. Fig. 7 shows the resulting curves for an electrode of the manufactured MEA.

In general, many materials exhibit a capacitive response in parallel with the resistive response, which is typical for metal – electrolyte interface. In Bode plot, as the spectrum has the impedance module at different frequencies, it is possible to identify whether the tested electrode has capacitive behavior, which is the situation in which it is perceived an impedance increase with decreasing frequency [38].

Amplitude of the impedance in the high frequency band is practically independent thereof its value corresponds only to the solution resistance (between medium and reference electrode), while for low frequency (becoming dependent of the frequency) the impedance appears due to the resistance polarization of the sample in solution (charge transfer and solution resistance). While iridium oxide electrodes the impedance becomes dependent on the frequency below 0.5 Hz, for TiN this limit is 4 kHz (ranging of 80 to 250 kΩ, about an order of magnitude lower than gold electrodes). In this value, the amplitude indicates the capacitive load as dominant current flux process [20, 33, 39].

Moreover, impedance phase is also frequency - dependent. At high frequencies, phase is close to zero, suggesting resistive impedance. In central region of the frequency range in the curve, phase tends to -90º, indicating a capacitive element (in this case, the interface capacitance) while at low frequencies, phase tends to back to zero. Comparatively, TiN has a more capacitive response at a higher frequency than IrOx [16, 33].
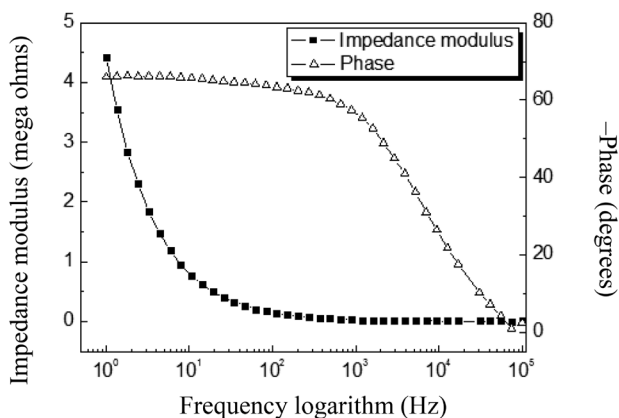
If the impedance modulus is contained within the range of 1 kΩ to 1 MΩ, decaying as the frequency increases, and phase is constant around 80º maximum, then the microelectrode is considered functional. Electrodes with impedances above 1 MΩ have higher noise level and exhibit a decrease in signal to noise ratio [40]. For short – circuited electrodes, this modulo will always be close to zero, regardless of frequency. However, if the electrodes are open, this module tends to infinity, regardless of the frequency [19].

In the study of Norlin & Leygraf (2002) [38], electrodes composed of various materials (platinum, titanium, titanium nitride) were tested by IS in saline. Platinum electrodes exhibited a low capacitance (6.0 x 10^{-5} F/cm²) and high charge transfer resistance (2.2 x 105 Ωcm²), with CEP lesser than 1, indicating there was a deviation from the ideal capacitive response.

Remaining material showed a significantly higher capacitance with lower polarization resistance. Despite that, titanium presents a high initial capacitance (1.6 x 10^{-4} F/cm²). This value may reduce over time, since an oxide film is created spontaneously on the titanium layer. Titanium nitride, however, showed higher capacitance and resistance (3.5 x 10^{-2} F/cm² and 6.4 x 10^3 Ωcm²). Based on all results, it was concluded that one way to increase the capacitance and minimize the charge transfer resistance is to increase the effective surface area of the electrode, which in turn improves their ability to stimulate and/ or register signs. As solutions there are the depositions of (1) TiN on Ti and Pt/Ir films, which makes the effective area of the order of several hundred times higher, and (2) Pt on Ti film. This is due to the fact that Pt significantly increases the effective area and by the TiN roughness [38].

In the study of Weiland et al. (2002) [35], which compared the response of iridium oxide and TiN electrodes, the first one showed a higher CSC, except in high frequency. When frequency has exceeded 10 kHz, the measured im-pedance was 15% higher than the second material.

Regarding to impedance measurements, research of Janders et al. (1996) [41] found very different values comparing TiN, gold and iridium (deposited by Sputtering) electrodes with an area of 80 μm², whose levels were 150kΩ, 2900 kΩ and 100 – 750 kΩ, respectively. Thus, the authors claim that TiN was a better choice than IrOx, with respect to the mechanical and electrical properties. TiN also has a higher charge injection safe limit and lower impedance despite lower charge capacity compared to iridium. Consequently, the material TiN is well suited for extracellular stimulation and neural activity recording.

When compared to literature, our MEA showed good results. Impedance average at 1 kHz for the electrodes considered good was ~142 kΩ. This value is

Figure 7. Results derived from Impedance Spectroscopy referring to a microelectrode of our MEA. Impedance modulus (black symbol) and phase angle (white symbol) curves are plotted as a function of frequency logarithm. Initially, at low frequencies, both impedance module and phase (approaching -80º) are high, decreasing as the frequency is increased. At high frequencies, phase is close to zero, suggesting resistive impedance.

close to the range obtained by Egert et al. (1998) [20]. With TiN electrodes of the same diameter, they were able to measure impedance ranging from 80 to 250 kΩ, whose magnitude is about an order of magnitude smaller than the impedance seen in planar gold electrodes. Furthermore, for our device, results are very close to those found for impedance spectroscopy at the MEA from MultiChannel Systems, which shows impedance values in the range of 30 – 400 kΩ.

Comparing our results to the literature, the main contribution of this work is focused in the MEA fabrication, which was fully manufactured in Brazil employing 100% of local technology, as follows.

a) Insulation layer

In the literature, MEAs are often passivated with silicon– based materials, such as SiO_2 [42 – 44], Si_3N_4 [20, 45, 46], and $SiO_2 – Si_3N_4 – SiO_2$ composite [10, 17], involving thickness up to 100 nm. In order to accomplish this task, this insulation material must be fully capacitive, so there is no leakage current or any other conductivity clue [10]. According to (1), the thickness of the material used in the insulation layer does influence this capacitance. Thus, in order to achieve a suitable insulation, a thicker layer is desirable [17, 47, 48]. In this context, a possible option is to employ polymers (such as polyimide, SU – 8), that can be implemented with up to several micrometers of thickness, and consists of photosensitive materials. In consequence, this enables simple and low cost patterning. Therefore, in order to ensure proper insulation, instead of using a single thick layer based on SiO_2, we decided to use two layers: SiO_2 and SU – 8. Among the advantages of the latter, we can highlight its transparency, high chemical stability and biocompatibility [10, 49, 50].

b) Interlayer

We have performed a step that is not present in most studies [10, 36, 51]: the interlayer, which we consider mandatory in order to implement an efficient device. The presence of this layer on MEA will assure that possible contaminants arising from the substrate are minimized, therefore avoiding the damage of the culture plated on the MEA, as well as improving the adhesion between substrate and conductive layer.

IV. CONCLUSIONS

This paper presented the production and characterization of 60 – channel MEAs, with TiN microelectrodes on glass substrate and insulation of SiO_2 and SU – 8, for use in neural cell cultures, completely manufactured in Brazil.

Experimental analysis pointed out that our MEA yields very good performance. Best electrodes in our MEA presented very good sensitivity to noise, leading to amplitudes of $10\mu V_{p-p}$, with RMS value of 2.6 μV. During stimulation test, signals recorded at microelectrodes yielded a waveform very close to the ECG injected by the function generator, but with lower amplitude (which is expected). In addition, regarding the Cyclic Voltammetry, resulting curves of our MEA presented similar shapes to the commercial device, but with higher current density (about an order of magnitude higher), with high CSCc amplitude (0.63 mC.cm^{-2}, with a potential window of –1 V to +1 V), which may be considered a reasonable result. Finally, Impedance Spectroscopy depicted that the impedance of our electrodes (~41kΩ at 1 kHz) is very close to those found in commercial devices. Moreover, due to the qualities of the conductor used (such as high charge injection safe limit and low impedance), TiN may be considered an interesting, adequate option for extracellular stimulation and neural activity recording.

Hence, based on all these tests and considerations, we can conclude that we have successfully developed both masks and process steps, as in the implementation of MEAs with functional microelectrodes. Results arising from testing the device reported in this work are within the expected range and compatible to standard commercial MEAs, so they are suitable for MEA applications.

ACKNOWLEDGEMENTS

REFERENCES

[1] M. Chiappalone, A. Vato. M. B. Tedesco, M. Marcoli, F. Davide, and S. Martinoia, "Networks of neurons coupled to microelectrode arrays: a neuronal sensory system for pharmacological applications.," Bionsen. Bioelectron., vol. 18, no. 5 – 6, May, 2003, pp. 627 – 634.

[2] W. B. F. Rieke, D. Warland, R. R. van Steveninck, *Spikes: exploring the neural code*, Cambridge, MA: The MIT Press, 1997, pp. 234.

[3] S. Martinoia, L. Bonzano, M. Chappalone, and M. Tedesco, "Electrophysiological activity modulation by chemical stimulation in networks of cortical neurons coupled to microelectrode arrays: a biosensor for neuropharmacological applications," Sensors Actuators B Chem., vol. 18, no. 1 – 2, Jul., 2005, pp. 589 – 596.

[4] R. E. Hampson, J. D. Simeral, and S. A. Deadwyler, "Distribution of spatial and nonspatial information in dorsal hippocampus," Nature, vol. 402, no. 6762, Dec., 1999, pp. 610 – 614.

[5] R. Madhavan, Z. C. Chao, and S. M. Potter, "Plasticity of recurring spatiotemporal activity patterns in cortical networks," Phys. Biol., vol. 4, no. 3, Sep., 2007, pp. 181 – 193.

[6] C. L. Torborg, K. A. Hansen, and M. B. Feller, "High frequency, synchronized bursting drives eye – specific segregation of retino - geniculate projections," Nat. Neurosci., vol. 8, no. 1, Jan., 2005, pp. 72 – 78.

[7] P. A. Friedmann, "Novel mapping techniques for cardiac electrophysiology," Heart, vol. 87, no. 6, Jun., 2002, pp. 575 – 582.

[8] S. M. Potter and T. B. DeMarse, "A new approach to neural cell culture for long – term studies," J. Neurosci. Methods, vol. 110, no. 1 – 2, Sep., 2001, pp. 17 – 24.

[9] Y. H. Tennico, M. T. Koesdjojo, S. Kondo, D. T. Mandrell, and V. T. Remcho, "Surface modification – assisted bonding of polymer – based microfluidic devices," Sensors Actuators B. Chem., vol. 143, no. 2, Jan., 2010, pp 799 – 804.

[10] M O. Heuschkel, C. Wirth, E. Steidl, and B. Buisson, "Development of 3D multielectrode arrays for use with acute tissue slices," in Advances in network electrophysiology using multielectrode arrays, M. Taketani; M. Baudry, Ed. New York, NY: Springer Science+Business Media, Inc., 2006, pp. 69 – 111.

[11] D. A. Borkholder, J. Bao, N. I. Maluf, E. R. Perl, and G. T. Kovacs, "Microelectrode arrays for stimulation of neural slice preparations," J. Neurosci. Methods, vol. 77, no. 1, Nov., 1997, pp. 61 – 66.

[12] Q. Dai, R. Rajasekharan, H. Butt, K. Won, X. Wang, T. D. Wilkinson, and G. Amaragtunga, "Transparent liquid – crystal – based microlens arrays using vertically aligned carbon nanofiber electrodes on quartz substrates," Nanotechnology, vol. 22, no. 11, Mar., 2011, pp. 115 – 201.

[13] S. A. Boppart, B. C. Wheeler, and C. S. Wallace, "A flexible perforated microelectrode array for extended neural recordings," IEEE Trans. Biomed. Eng., vol. 39, no. 1, Jan., 1992, pp. 37 – 42.

[14] S. Khan, A. Mian, and G. Newaz, *Thin films and coatings in biology*, S. Nazarpour, Ed. Dordrecht, Springer: 2013, pp. 301 – 330.

[15] A. Hai, J. Shappir, and E. Spira. "Long-term, multisite, parallel, in-cell recording and stimulation by an array of extracelular microelectrodes," J Neurophysiol., vol. 104, 2010, pp. 559 – 568.

[16] W. Franks, I. Schenker, P. Schmutz, and A. Hierlemann, "Impedance characterization and modeling of electrodes for biomedical applications," IEEE Trans. Biomed. Eng., vol. 52, no. 7, Jul., 2005, pp. 1295 – 1302.

[17] K. Wang, "A carbon nanotube microelectrode array for neural stimulation," Stanford University, 2006.

[18] M. Systems, "Microelectrode array (MEA) manual," Reutlingen, 2015, pp. 1 – 131.

[19] S. F. Cogan, "Neural stimulation and recording electrodes," Annu.Rev. Biomed. Eng., vol. 10, Jan., 2008, pp. 275 – 309.

[20] U. Egert, B. Schlosshauer, S. Fennrich, W. Nisch, M. Fejtl, T. Knott, T. Müller, and H. Hämmerle, "A novel organotypic long – term culture of the rat hippocampus on substrate – integrated multielectrode arrays," Brain Res. Protoc., vol. 2, no. 4, Jun., 1998, pp. 229 – 242.

[21] M. Martínez-Gutiérrez, and J. E. Castellanos, "Morphological and biochemical characterisation of sensory neurons infected in vitro with rabies virus," Acta Neuropathol., vol. 114, 2007, pp. 263 – 269.

[22] K. E. Petersen, "Silicon as a mechanical material," in Proceedings of the IEEE, 1982, pp. 420 – 434.

[23] S. M. Sze and K. K. Ng, *Physics of semiconductor devices*, 3rd ed. Hoboken, NJ: John Wiley & Sons, 2007, pp. 1 – 814.

[24] S. Wolf, *Silicon processing for the VLSI era* – Vol. 2: Process integration, Sunset Beach, CA: Lattice Press, 1990, pp. 1 – 782.

[25] J. Robertson, "High dielectric constant oxides," Eur. Phys. J. Appl. Phys., vol. 28, 2004, pp. 265 – 291.

[26] O. Toader, and S. John, "Proposed square spiral microfabrication architecture for large three – dimensional photonic band gap crystals," Science, vol. 292, no. 5519, 2001, pp. 1133 – 1135.

[27] R. Machorro, E. C. Samano, G. Soto, F. Villa, and L. Costa – Araiza, "Modification of refractive index in silicone oxynitride films during deposition," Materials Letters, vol. 45, 2000, pp. 47 – 50.

[28] J. Bergmann, M. Heusinger, G. Andrä, and F. Falk, "Temperature dependente optical properties of amorphous silicone for diode laser crystallization," Optics Express, vol. 20, no. 106, 2012, pp. A856 – A863.

[29] S. M. Potter, D. A. Wagenaar, and T. B. DeMarse, "Closing the loop: stimulation feedback systems for embodied MEA cultures," in *Advances in network electrophysiology: using multielectrode arrays*, M. Taketani, M. Baudry, Ed. New York, NY: Springer Science+Business Media, Inc., 2006, pp. 215 – 242.

[30] D. A. Wagenaar, R. Madhavan, J. Pine, and S. M. Potter, "Controlling bursting in cortical cultures with closed – loop multielectrode stimulation," J. Neurosci., vol. 25, no. 3, Jan., 2005, pp. 680 – 688.

[31] M. J. Madou, "Electrochemical and optical analytical techniques," in *Solid – state physics, fluidics, and analytical techniques in micro and nanotechnology*, vol. 1, Irvine, CA: CRC Press, 2011, pp. 552 – 555.

[32] C. G. Zoski, "Handbook of electrochemistry," Oxford, UK: Elsevier, 2007.

[33] W. Hasenkamp, S. Musa, A. Alexandru, W. Eberle, and C. Bartic, "Electrodeposition and characterization of iridium oxide as electrode material for neural recording and stimulation," in *World Congress on Medical Physics and Biomedical Engineering*, 2009, pp. 472 – 475.

[34] D. M. Zhou and R. J. Greenberg, "Electrochemical characterization of titanium nitride microelectrode arrays for charge – injection applications," in *25th Annual International Conference of the IEEE EMBS*, 2003, pp. 1964 – 1967.

[35] J. D. Weiland, D. J. Anderson, and M. S. Humayun, "In vitro electrical properties for iridium oxide versus titanium nitride stimulating electrodes," IEE Trans. Biomed. Eng., vol. 49, no. 12, Dec., 2002, pp. 1574 – 1579.

[36] N. P. Aryan, M. Imam, H. Bin, C. Brendler, S. Kibbel, G. Heusel, and A. Rothermel, "In vitro study of titanium nitride electrodes for neural stimulation," in *33rd Annual International Conference of the IEEE EMBS*, 2011, pp. 2866 – 2869.

[37] A. J. Bard, and L. R. Faulkner, "Techniques based on concepts of impedance," in Electrochemical methods: Fundamentals and applications. New York, NY: John Wiley & Sons, Inc., 2001, pp. 368 – 416.

[38] A. Norlin, J. Pan, and C. Leygraf, "Investigation of interfacial capacitance of Pt, Ti and TiN coated electrodes by electrochemical impedance spectroscopy," Biomol. Eng., vol. 19, 2002, pp. 67 – 71.

[39] F. Heer, W. Franks, A. Blau, S. Taschini, C. Ziegler, A. Hierlemann, and H. Balter, "CMOS microelectrode array for the monitoring of electrogenic cells," Biosens. Bioelectron., vol. 20, 2004, pp. 358 – 366.

[40] M. O. Heuschkel, M. Fejtl, M. Raggenbass, D. Bertrand, and P. Renaud, "A three – dimensional multi – electrode array for multisite stimulation and recording in acute brain slices," J. Neurosci. Methods, vol. 114, no. 2, Marc., 2002, pp. 135 – 148.

[41] M. Janders, U. Egert, M. Stelzle, and W. Nisch, "Novel thin film titanium nitride microelectrodes with excellent charge transfer capability for cell stimulation and sensing applications," in *18th Annual International Conference of the IEEE Engineering in Medicine and Biology Society*, 1996, pp. 245 – 247.

[42] R. Kim, S. Joo, H. Jung, N. Hong, and Y. Nam, "Recent trends in microelectrode array technology for in vitro neural interface platform," Biomed. Eng. Lett., vol. 4, 2014, pp. 129 – 141.

[43] A. Blau, *Prospects for neuroprosthetics: Flexible microelectrode arrays with polymer conductors*, in Applied Biomedical Engineering, G. D. Gargiulo, and A. McEwan (Ed.), ISBN: 978 – 953 – 307 – 256 – 2, InTech: 2011, pp. 83 – 123.

[44] R. Kiran, L. Rousseau, G. Lissorgues, E. Scorsone, A. Bongrain, B. Yvert, S. Picaud, P. Mailley, and P. Bergonzo, "Multichannel boron doped nanocrystalline diamond ultramicroelectrode arrays: Design, fabrication and characterization," Sensors, vol. 12, 2012, pp. 7669 – 7681.

[45] H. Charkhkar, G. L. Knaack, B. E. Gnade, E. W. Keeder, J. J. Pancrazio, "Development and demonstration of a disposable low – cost microelectrode array for cultured neuronal network recording," Sensors and Actuators B., vol. 161, Nov. 2011, pp. 655 – 660.

[46] K. C. Cheung, K. Djupsund, Y. Dan, and L. P. Lee, "Implantable multichannel electrode array based on SOI technology," Journal of Microelectromechanical Systems, vol. 12, no. 2, April 2003, pp. 179 – 184.

[47] A. M. H. Ng, Y. Wang, W. C. Lee, C. T. Lim, K. P. Loh, and H. Y. Low, "Patterning of graphene with tunable size and shape for microelectrode array devices," Carbon, vol. 67, 2014, pp. 390 – 397.

[48] C. A. Rusinek, M. F. Becker, R. Rechenber, and T. Schuelke, "Fabrication and characterization of boron doped diamond microelectrode arrays of varied geometry," Electrochemistry Communications, vol. 73, 2016, pp. 10 – 14.

[49] G. Márton, G. Orbán, M. Kiss, A. Pongrácz, and I. Ulbert, "A novel polyimide – platinum – SU-8 microelectrode array for various electrophysiological applications," Procedia Engineering, in Eurosensors 2014, the 28th European Conference on Solid – State Transducers, vol. 87, 2014, pp. 380 – 383.

[50] L. Berdondini, M. Chiappalone, P. D. van der Wal, K. Imfeld, N. F. de Rooij, M. Koudelka – Hep, M. Tedesco, S. Martinoia, J van Pelt, G. Le Masson, and A. Garenne, "A microelectrode array (MEA) integrated with clustering structures for investigating in vitro neurodynamics in confined interconnected sub – populations of neurons," Sensors and Actuators B: Chemical, vol. 14, no. 1, March 2006, pp. 530 – 541.

[51] A. Czeschik, A. Offenhäusser, and B. Wolfrum, "Fabrication of MEA – based nanocavity sensor arrays for extracellular recording of action potentials," Phys. Status Solidi.A, vol.211, no. 6, 2014, pp. 1462 – 1466.